

Electronic Supporting Information

Augmented Band Gap Tunability in Indium-Doped Zinc Sulfide Nanocrystals

Enrico Della Gaspera^{a,*}, *Joseph Griggs*^a, *Taimur Ahmed*^b, *Sumeet Walia*^b, *Edwin L. H. Mayes*^c,
Arrigo Calzolari^d, *Alessandra Catellani*^d, *Joel van Embden*^{a,*}

^a School of Science, RMIT University, Melbourne VIC 3000, Australia

^b Functional Materials and Microsystems Research Group and Micro Nano Research Facility,
RMIT University, Melbourne VIC 3000, Australia

^c RMIT Microscopy and Microanalysis Facility, School of Science, RMIT University, Melbourne
VIC 3000, Australia

^d Istituto Nanoscienze CNR-NANO Centro S3, 41125 Modena, Italy

Corresponding authors: *enrico.dellagaspera@rmit.edu.au, joel.vanembden@rmit.edu.au

Additional Experimental details

The patterns for the inter-digitated electrodes were created on Si substrates covered with 100 nm SiO₂: a photoresist layer was deposited by spin coating and dried at 100 °C, exposed to UV light through a mask using a mask aligner system (MA6, SUSS MicroTech) which defined the patterns, and subsequently developed. The Cr/Au metal electrodes (10/100 nm) were then deposited on the developed patterns using electron beam evaporation. Finally, the lift-off in acetone was carried out to reveal the required metallic contact pads for micro-probes and electrical measurement.

Figure S1

XRD patterns for ZnS nanocrystals doped with 20% indium synthesized at different temperatures. An impurity peak centered at ~23° and a shoulder at ~47°, tentatively ascribed to indium oxide (ICDD No. 22-0336), indium sulfide (ICDD No. 86-0640) or indium zinc sulfide (ICDD No. 79-0766) is observed in the sample synthesized at 60 °C, while samples synthesized at higher temperatures show only pure phase ZnS. In addition, a sharpening of the diffraction peaks with increasing reaction temperature can be observed.

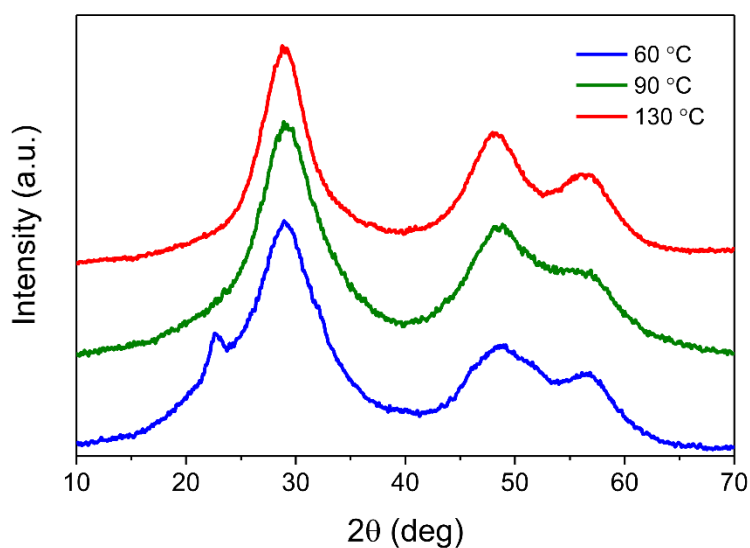


Figure S2

Experimental XRD data (open circles), fitted peaks (shaded curves) and sum of all fittings (red line) for a typical ZnS sample. The difference between experimental data and the fitting is reported at the bottom as a grey line. The fitting has been done to precisely calculate the full width at half maximum to evaluate the crystallite size using the Scherrer formula.

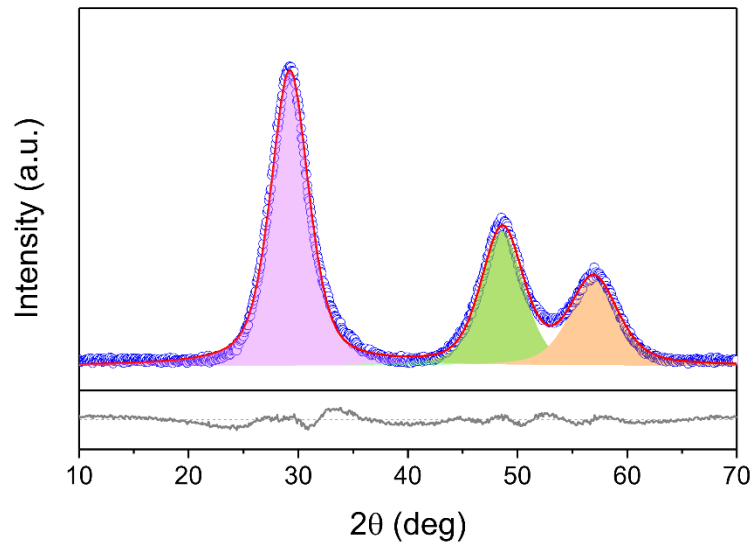


Figure S3

Predicted lattice constant a for a cubic ZnS cell (bulk) as a function of the amount of indium dopant added substitutional to zinc.

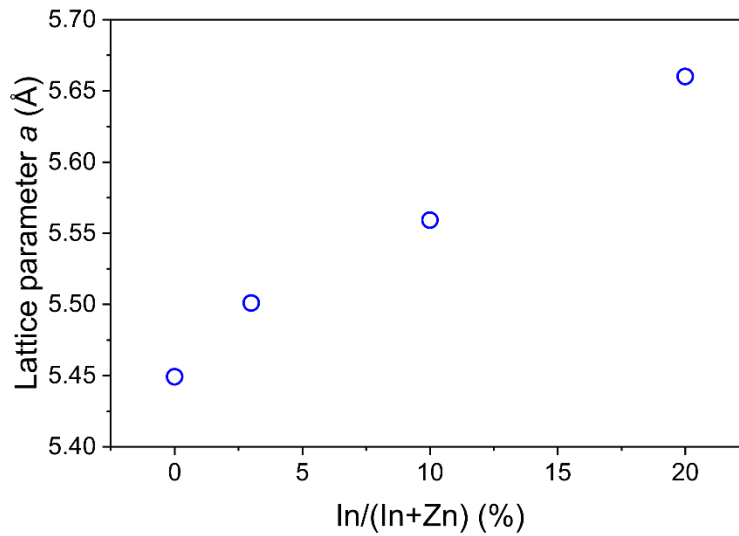
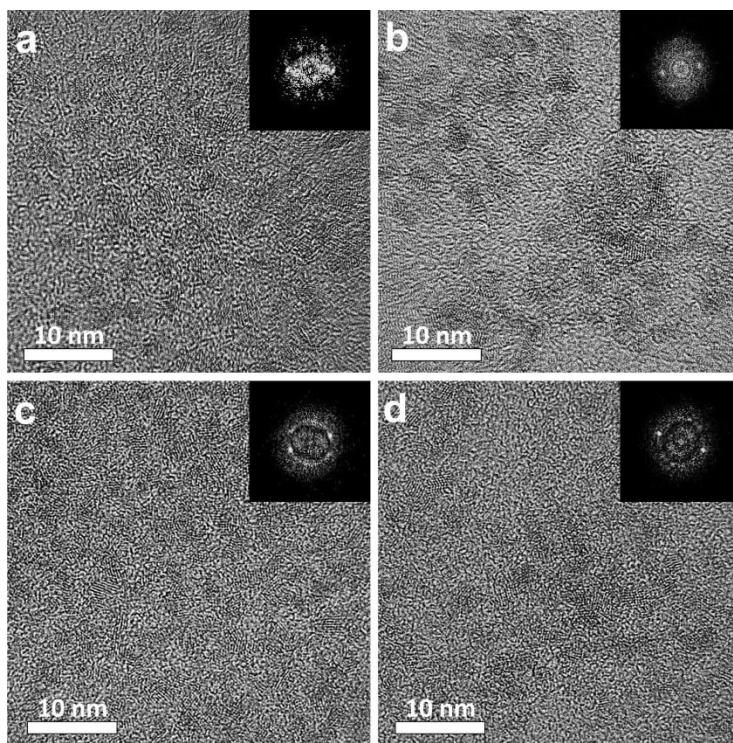


Figure S4

Additional TEM images and respective Fast Fourier Transform (FFT) for both undoped (a) and doped (5%, b; 10%, c; 20%, d) ZnS NCs synthesized at 130 °C.

**Figure S5**

Lattice spacing corresponding to the (111) crystalline plane obtained from FFT analysis of various high-resolution TEM images of ZnS NCs with increasing indium doping.

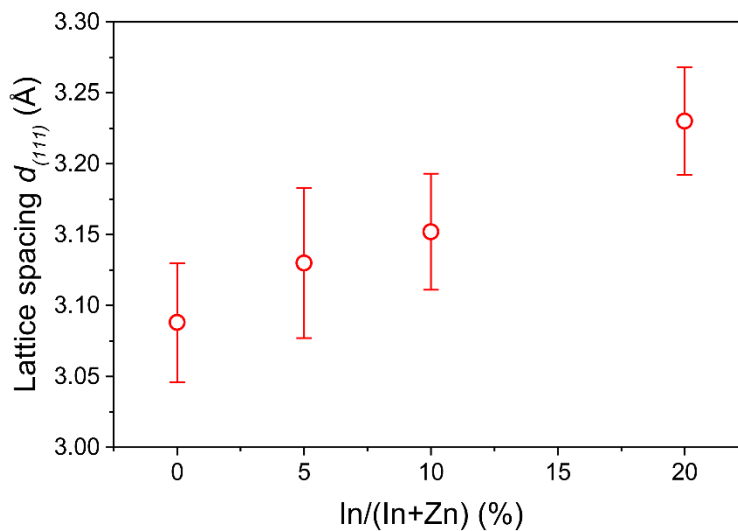


Figure S6

Absorbance (dashed lines) and PL (straight lines) for undoped ZnS NCs synthesized at different temperatures. Compared to Figure 3a, this plot shows only a zoomed view of the PL spectra, to highlight the weak band-to-band emission, which appears as a shoulder in the emission spectra in correspondence to the absorption onset (band gap) of ZnS NCs.

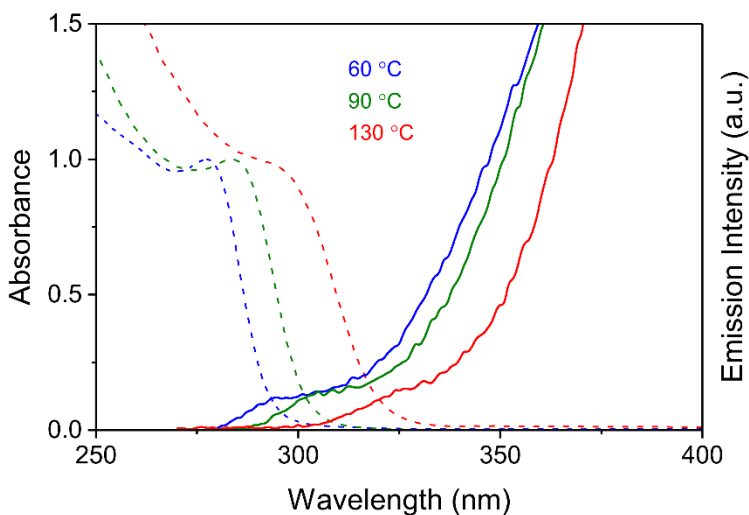


Figure S7

Band gap values as a function of crystallite size for samples synthesized at various doping levels and reaction temperatures. The dashed lines are just a guide to the eye to identify samples with the same doping level.

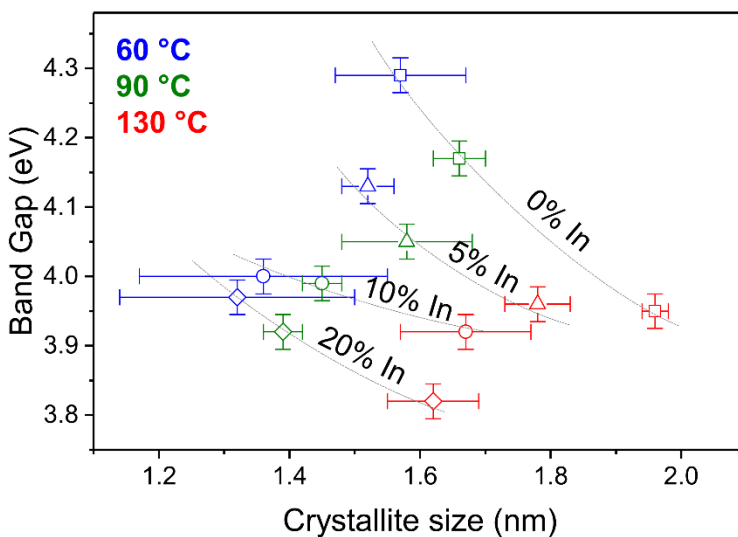


Figure S8

Predicted band gap energy for undoped and indium-doped bulk ZnS obtained from first principles simulations.

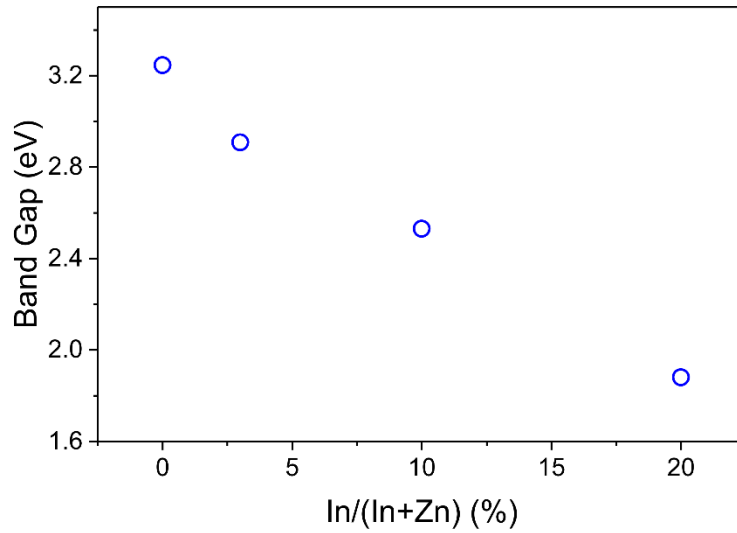


Figure S9

DOS for In-doped ZnO at In = 3% substitutional at Zn sites. The top of the valence band for the undoped host bulk is taken as energy reference ($E = 0$ eV). The grey box represents the pristine band gap of the host.

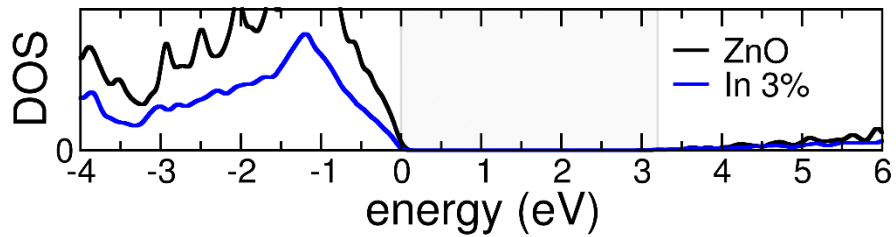


Figure S10

The imaginary component of the complex dielectric function for undoped (black) and doped (red) ZnS.

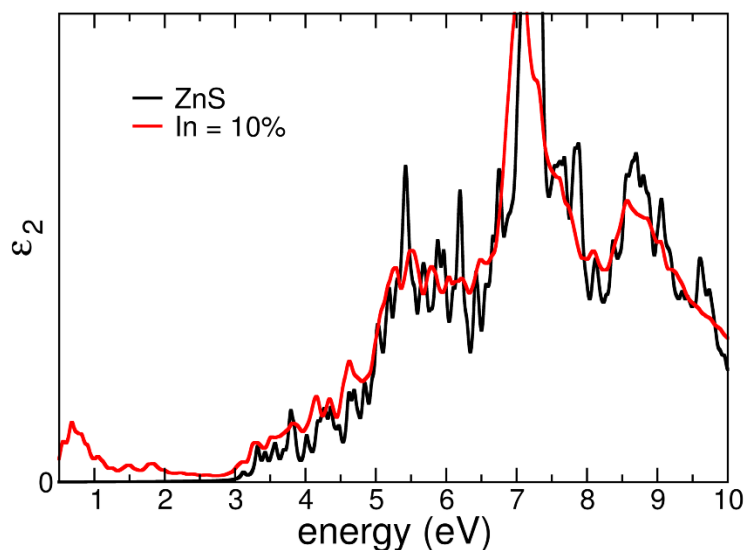


Figure S11

Absorption spectra in the UV-Vis-NIR for In-doped ZnS synthesized in this study and In-doped ZnO prepared according to [1]. In-doped ZnO shows a clear plasmon resonance in the near IR region, while In-doped ZnS are completely transparent.

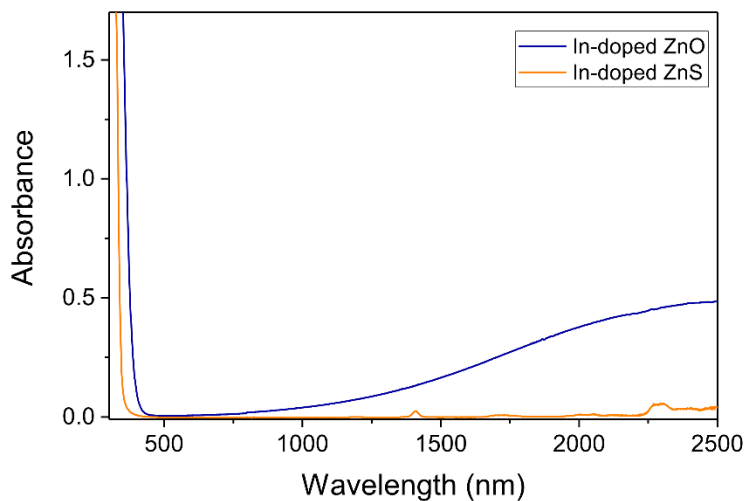


Figure S12

Sketch of band alignment between ZnO, ZnS, and the ionization potential of atomic In (taken as reference with $E = 0$ eV) as evaluated by *ab initio* simulations. Calculations for ZnO and ZnS are performed in supercells of 192 atoms, with 28 (280) Ry cutoff for wave functions (charge density), US pseudopotentials, and only the Gamma point sampling. Similarly, the ionization potential of In was evaluated in a single atom supercell, with the same samplings.

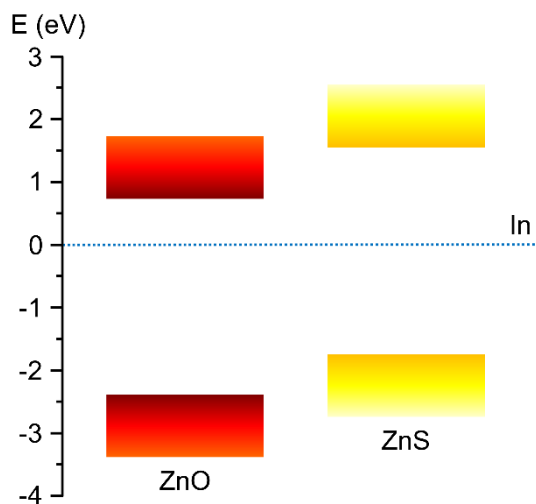
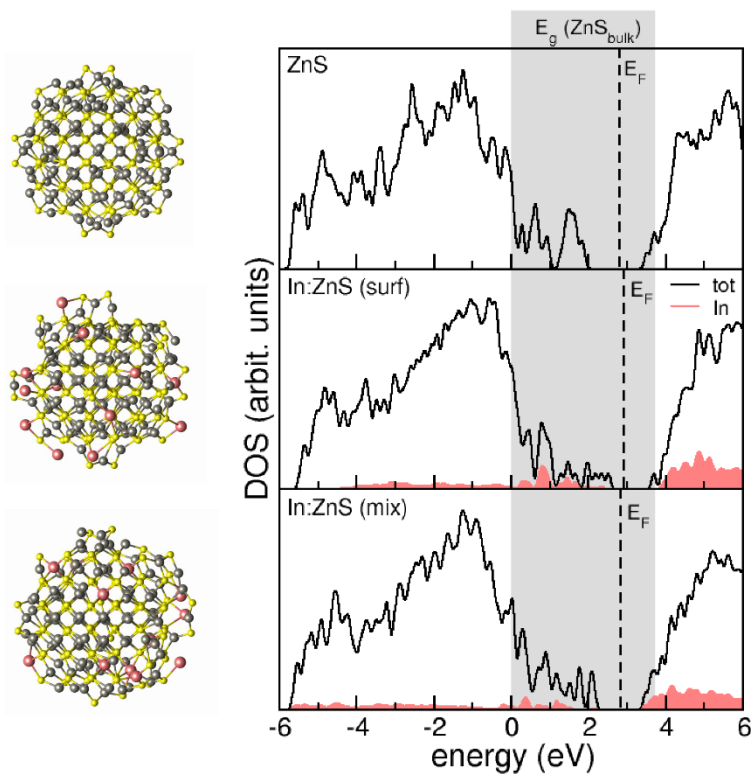


Figure S13

Relaxed configuration for three ZnS NC models and their corresponding DOS: undoped ZnS NC (top); *surf* configuration (middle) and *mix* configuration (bottom). See discussion below for details.



We further performed simulations for doped ZnS NCs: calculations were performed for three different NC structures, namely undoped ZnS; NC with 10% In substitutional doping at Zn surface sites (*surf*); and NC with 10% In substitutional doping at Zn sites, where In atoms lay both within the NC and at the NC edges (*mix*). NC size was kept constant at 2 nm. We performed a First Principles Molecular Dynamics (FPMD) run on a (32x32x32) Å³ box with the CP code (also included in the Quantum Espresso suite), 28 Ry energy cutoff and Γ sampling; samples were first heated for 1 ps at 390 K, close to the experimental growth conditions; we then allowed for full atomic and electronic relaxation towards the minimum energy-and-force structure. Although this simulation time is too short to investigate diffusive phenomena, the initial FPMD run allowed to randomize and subsequently optimize the NC geometry. The configuration with In atoms at the NC surface is more stable by ~ 6.8 eV/NC (0.6 eV/In atom) than configuration *mix*. This is mostly due a better accommodation of the larger In atoms (with respect to Zn). In fact, the steric hindrance of indium atoms deep within the NC causes large stresses and subsequent increase in the lattice parameter, as discussed in the main text. When In inclusions are located at the surface, the NC has more degrees of freedom to accommodate the stress, as it is evident in the optimized structures of Figure S13. This reduces the total energy of the system. The preference of In adatom to reside on surfaces is a quite general conditions observed for many other semiconductor systems (see supporting references 2-4).

The results of the electronic structure are summarized in Figure S13, where we show the density of states (DOSs) of the considered NCs. Even the undoped ZnS NC exhibits in-gap states (IGSs) induced by unsaturated surface dangling bonds (DBs). Notably, this results in a reduction of the effective band-gap with respect to the bulk crystal, which compensates the bandgap opening induced by quantum confinement. This seems to be in contrast with experimental findings (both by us and others), but the inconsistency is only apparent. We remark, indeed, that NC simulations are performed in vacuum, i.e. without any embedding environment or impurity that can passivate the highly reactive DBs of ZnS NCs. Saturation of surface states stabilizes the NC structure opening the bandgap, to recover the value expected for undoped NCs. The inclusion of In during NC growth does not passivate the DBs, as it is a substitutional dopant (since In forms alternative bonds with S in place of Zn, it does not saturate the surface states). As a consequence, the inclusion of In does not restore the bandgap of the ZnS crystal. The DOS of In:ZnS in *surf* and *mix* configuration are thus very similar and dominated by the presence of both In-derived and surface IGSs, where the differences between the two structures are ascribed to the details of single In-S bonds. With respect to the bulk single crystal described in the main text, here the different In-S coordination patterns (see Figure S13) give rise to a series of occupied states instead of the unique band observed in the bulk, that further reduces the band gap.

Figure S14

Dispersion curves for refractive index and extinction coefficient measured with spectroscopic ellipsometry for various ZnS film. The refractive index (n) and absorption coefficient (k) were evaluated from the experimental Ψ (psi) and Δ (delta) values using the CompleteEase software package, fitting the experimental data with Cauchy dispersion and Tauc-Lorentz oscillators for the non-absorbing region and UV absorption edge, respectively.

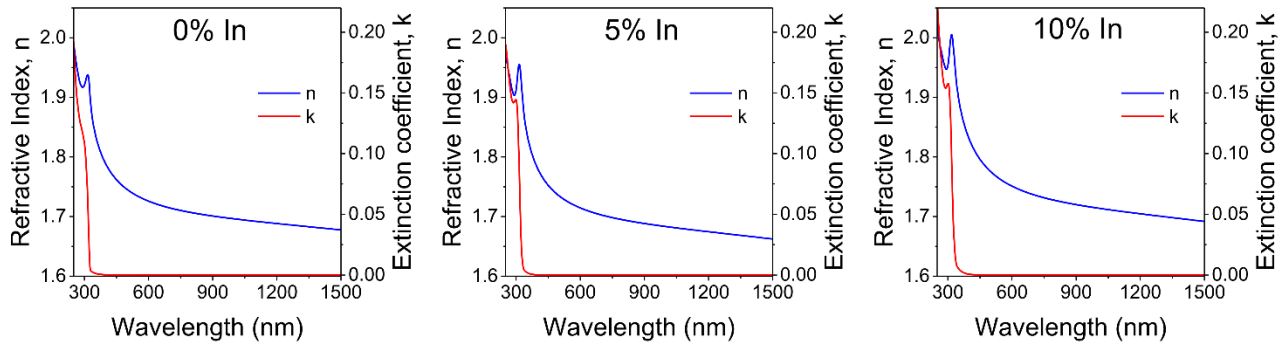


Figure S15

SEM images in top view at different magnifications of a ZnS:In (10%) thin film

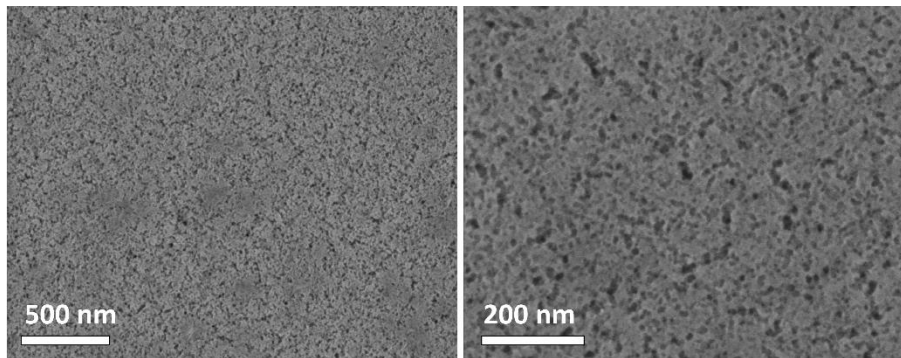
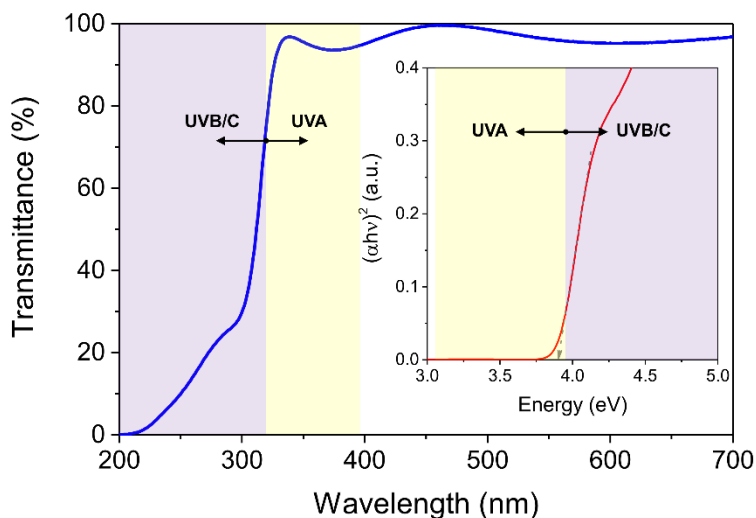


Figure S16

Optical transmittance spectrum of a doped ZnS film deposited on quartz showing high transparency in the visible range and a sharp UV absorption onset, in correspondence to the UVB energy range. The spectrum has been corrected for the absorption of the quartz substrate, and the presence of interference fringes confirms the excellent optical quality of the prepared coating. The inset shows the corresponding Tauc plot.

**Table S1**

Crystallite size evaluated from XRD patterns using the full width at half-maximum of the three main ZnS peaks. For each sample the three obtained values were averaged, and the error represents one standard deviation. The crystallite size increases with increasing reaction temperature, while Indium doping induces a progressive reduction in size, as highlighted by the “Variation” columns.

<i>Nominal</i> <i>In/(Zn+In) %</i>	60 °C		90 °C		130 °C	
	<i>Crystallite size (nm)</i>	<i>Variation (%)</i>	<i>Crystallite size (nm)</i>	<i>Variation (%)</i>	<i>Crystallite size (nm)</i>	<i>Variation (%)</i>
0	1.57±0.10	0	1.66±0.04	0	1.96±0.02	0
5	1.52±0.04	3	1.58±0.10	5	1.78±0.05	9
10	1.36±0.19	13	1.45±0.03	13	1.67±0.10	15
20	1.32±0.18	16	1.39±0.03	16	1.62±0.07	17

Table S2

Comparison of nominal (amount of precursor used) and experimental (from EDX) indium doping as a function of the reaction temperature for some of the samples synthesized in this study.

<i>Reaction temperature (°C)</i>	<i>Nominal In/(Zn+In) %</i>	<i>Experimental In/(Zn+In) %</i>	<i>Variation In/(Zn+In) %</i>
90	5	5.5 ± 1.3	+ 0.5
90	10	9.9 ± 1.0	- 0.1
130	0	0.8 ± 0.5 ^a	+0.8
130	5	6.3 ± 0.8	+ 1.3
130	10	9.7 ± 1.5	- 0.3

^a This value is indicative of the noise in the EDX spectra and it is not reflective of the actual In concentration.

Supporting references

- [1] E. Della Gaspera, A. S. R. Chesman, J. van Embden, J. J. Jasieniak, *ACS Nano*, **2014**, *8*, 9154.
- [2] J. H. Cho, S. B. Zhang, A. Zunger, *Phys. Rev. Lett.*, **2000**, *84*, 3654.
- [3] G. B. Stringfellow, *J. Cryst. Growth.*, **2010**, *312*, 735.
- [4] A. I. Duff, L. Lymperakis, J. Neugebauer, *Phys. Rev. B*, **2014**, *89*, 085307.